INORGANIC CHEMISTRY
FRONTIERS

RESEARCH ARTICLE

View Article Online
View Journal | View Issue

Cite this: *Inorg. Chem. Front.*, 2022, **9**, 4394

Fluorescence analysis for characterizing the alkali stability of metal–organic frameworks: an informative complement to X-ray diffraction†

Shuai-Liang Yang,[a] Gen Li,[a] Xiao-Yan Liu,[a] Lin Zhang,[a] Yan Xu[a] and En-Qing Gao *[a,b]

Received 30th April 2022,
Accepted 4th July 2022

DOI: 10.1039/d2qi00949h

rsc.li/frontiers-inorganic

The stability of metal–organic frameworks (MOFs) in solutions is of essential importance from the perspectives of scientific research and practical applications. Powder X-ray diffraction (PXRD) with isolated solids is a common protocol to judge the stability. However, solid-state characterization may lead to ignorance of possible chemical leaching and even partial collapse, and the ignorance may lead to confusing or even false conclusions about stability and relevant properties. Herein, based on the pH-responsive fluorescence associated with alkaline hydrolysis of MOFs, a fluorometric method is proposed for characterizing the stability of luminescent or luminogenic MOFs in basic solutions. Exemplified by two Zr(IV) MOFs, Zr–TCPBP (tetracarboxylate linker) and UiO-66-NH_2 (dicarboxylate), the method has been validated by a comparative study with solid-state characterization using PXRD, scanning electron microscopy (SEM) and thermogravimetry. The method has the advantages of facile operation, high sensitivity and good complementarity to PXRD and SEM. It can be used to continuously monitor the whole hydrolytic process starting with nondestructive local hydrolysis and ending with abrupt and destructive hydrolysis, giving the pH values for different hydrolytic stages. The method has great potential to be extended for characterizing the stability of MOFs towards acids or other substrates in solution.

Introduction

Metal–organic frameworks (MOFs), an emerging kind of porous material built from metal nodes and organic links,[1–3] have aroused great scientific interest. Their structural designability, diversity, tunability, and porosity endow MOFs with potential applications in gas adsorption and separation,[4–7] chemical sensing,[8–14] photonics,[15,16] heterogeneous catalysis,[17–21] proton conduction,[22–25] *etc*. The functional performance of MOFs is highly dependent on their crystalline porous structures, and the structural lability to humidity, acids, bases and other external stimuli often limits their practical applications.[26,27] Thus, being aware of the stability/lability of MOFs under various conditions is very significant. Powder X-ray diffraction (PXRD) has been the conventional method to assess the structural integrity of MOFs isolated from solutions, but there are two important drawbacks of this method. One is that the possibility of partial leaching of MOF components without framework collapse is ignored. The other is that the amorphous materials generated by partial decomposition of MOFs may not be detected by PXRD. High-performance liquid chromatography (HPLC) has been used to detect leached ligands in aqueous solutions,[28,29] but the method needs tedious preliminary preparation and complex instrumentation. It is necessary to find a more effective method to complement PXRD for determining the stability of MOFs in solution.

Luminescent or luminogenic MOFs dispersed in solution often show sensitive emission changes in response to some chemical species. This has encouraged extensive studies to develop MOF-based chemical sensors with excellent sensitivity and selectivity having been reported.[30–35] Most studies attributed the fluorescence response to intact MOFs, the intactness being judged from PXRD with solids isolated from sensing media. The issue that the luminescence of MOF dispersions can be strongly affected by a minute amount of exuded fluorescent species is rarely addressed. The overlook may lead to erroneous conclusions and understandings.

Zr(IV) MOFs built from $Zr_6O_4(OH)_4$ nodes and carboxylate-terminated linkers are deemed to be a class of highly stable MOFs.[36,37] High acid resistance at pH < 0 has been commonly

[a]*Shanghai Key Laboratory of Green Chemistry and Chemical Processes, School of Chemistry and Molecular Engineering, East China Normal University, Shanghai 200062, China. E-mail: eqgao@chem.ecnu.edu.cn*
[b]*Institute of Eco-Chongming, Shanghai 202162, China*

†Electronic supplementary information (ESI) available: Experimental section and supplementary graphic materials, Fig. S1–S8. See DOI: https://doi.org/10.1039/d2qi00949h

reported,[38–41] which is understandable considering the well-matching double bonding of carboxylate groups with high oxophilic Zr_6 clusters and the low pK_a of aromatic –COOH.[27] However, the stability in basic solutions has been reported with great discrepancy even for the same MOF. Taking UiO-66-NH_2 as an example, Lillerud *et al.* reported that the MOF is completely decomposed into an amorphous phase after treatment with a pH 14 solution.[42] According to Van Der Voort *et al.*, the MOF maintains a good crystalline structure after placing in a pH 12 NaOH solution for two months.[43] However, Aguilera-Sigalat *et al.* showed that the MOF undergoes certain structural damage in alkaline solution with pH > 9.[44] These quite different conclusions are all based on PXRD analysis, reflecting the inadequacy of PXRD in characterizing the stability of MOFs in liquid media.

Herein, we developed a fluorometric method for determining the stability of MOFs in basic solutions. The method is based on the fluorescence response induced by alkaline hydrolysis of MOFs. By a comparative study combining PXRD, scanning electron microscopy (SEM) and thermogravimetry (TG), the feasibility and reliability of the method are first demonstrated with a Zr(IV) MOF (Zr–TCPBP) with 2,2′,6,6′-tetra(4-carboxyphenyl)-4,4′-bipyridine (TCPBP)[45] and then extended to UiO-66-NH_2 (Scheme 1). The method has the advantages of simple operation, high sensitivity and high informativeness, representing a nice complement to conventional solid-state characterization methods. In particular, it can be used to monitor the whole process from minor leaching of linkers to obvious hydrolysis and to complete hydrolysis, giving the pH range of rapid decomposition.

Results and discussion

Zr–TCPBP consists of 12-connected $Zr_6(\mu_3\text{-}O)_4(OH)_4(COO)_{12}$ and 4-connected $TCPBP^{4-}$ (Scheme 1). We previously demonstrated that the MOF has high acid stability and shows fluorescence transitions in the pH 3.3–1.8 region owing to cooperative protonation at the multiple basic pyridyl sites at pore surfaces.[45] In continuation of the previous work, we investigated its fluorescence response to high pH. As shown in Fig. 1, the fluorescence emission of a Zr–TCPBP dispersion in water (0.3 mg mL^{-1}, unless otherwise specified) shows no appreciable change in the wavelength or intensity in the range of pH 4.4–7.2. Upon further increasing the pH, the emission maximum is gradually blue shifted from 435 to 395 nm with a concomitant intensity increase.

On the one hand, the intensity initially increases smoothly, then abruptly rises in the range of pH 11.0–11.8, and finally becomes constant beyond the range (Fig. 1b). The critical point for the abrupt transition is at about pH 11.4, as estimated from the derivative curve. The intensity transition means that a small pH change can lead to a significant fluorescence enhancement, which indicates the potential application of the MOF as an ultrasensitive pH probe working in the highly basic range. On the other hand, the λ_{max} *vs.* pH plot shows two linearly dependent regions, a slow blue shift for pH varying from 7.5 to 9.6 and a rapid blue shift for pH 9.6–11.5 (Fig. 1c). The linear variation indicates the feasibility of quantitative pH determination in the basic range by monitoring λ_{max}. Fluorescence pH sensing based on wavelength shifts, compared to that based on intensity changes, can have some advantages such as high anti-interference and visual color changes.[46] Converting the emission spectra to chromaticity coordinates in the Commission Internationale de L'Eclairage (CIE) chromaticity diagram gives a linear region for pH 7.5–11.5, which corresponds to the cyan-to-blue change in the fluorescence color (Fig. S1†).

To explore the mechanism of the complex pH dependence of fluorescence in basic solutions, we filtered the Zr–TCPBP dispersions in pH 7.2, 9.6 and 11.5 solutions and measured the fluorescence of the filtrates and solid residues re-dispersed in water. The filtrate for the nearly neutral dispersion shows no emission, but those for pH 9.6 and 11.5 show significant emission, which is even more intense than the emission of the unfiltered dispersions (Fig. 2a). The latter two filtrates share the same λ_{max} (395 nm) with the free organic ligand dissolved in basic solution, indicating the presence of the ligand in the filtrates and also in the corresponding dispersions. That is, there is no leaching of the ligand for neutral dispersions, but significant leaching occurs for the dispersions of pH 9.6 and 11.5 because of hydrolysis of the MOF. The emission intensity of the pH 11.5 filtrate was significantly higher than that for pH 9.6, confirming the expectation that the degree of leaching or hydrolysis increases with pH. As can be seen, the pH 11.5 dispersion and its filtrate both have λ_{max} = 395 nm, and the emission intensity of the filtrate is very close to that of the ligand solution with a controlled concentration. This suggests almost complete MOF hydrolysis and ligand release at that pH. The fact that the emission of the dispersion is weaker than that of its filtrate can be simply because of the scattering effect of the solid particles in the dispersion. The conclusions are corrobo-

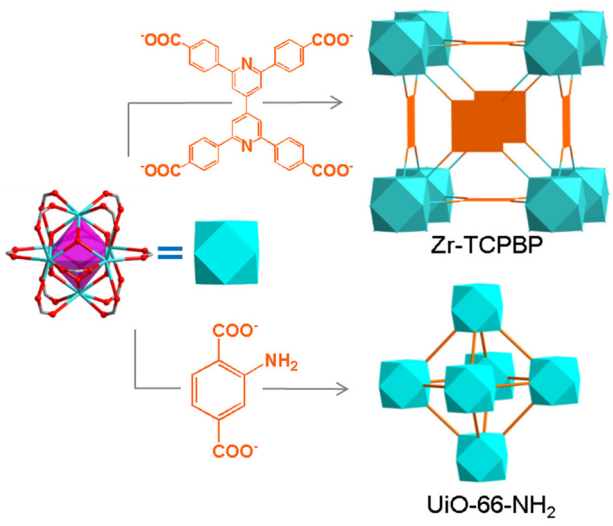

Scheme 1 Structures of the MOFs studied.

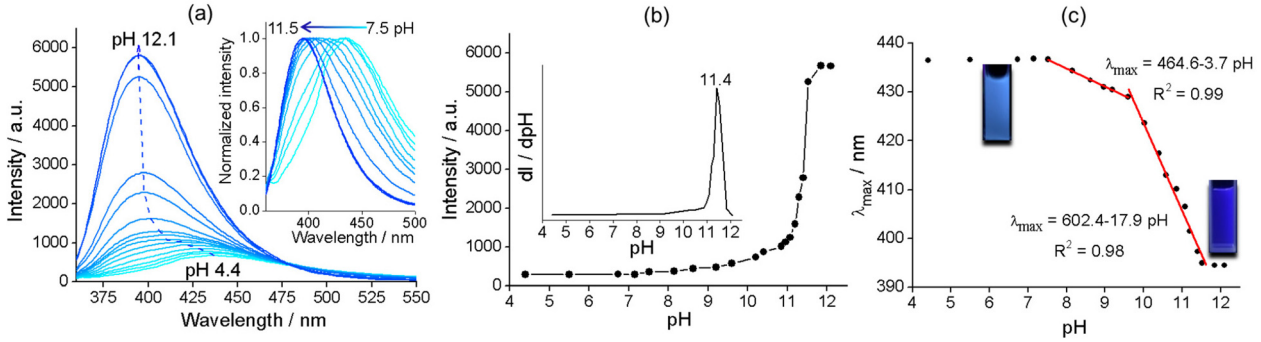

Fig. 1 (a) Emission spectra of the suspension of Zr–TCPBP in the pH 4.4–12.1 range under 345 nm excitation (the dashed arrow shows the trace of the emission maximum with increasing pH). The inset shows the intensity-normalized spectra at pH 7.5–11.5. (b) Variation of the emission intensity at 395 nm with pH. The inset shows the derivative plot. (c) pH dependence of the λ_{max} and the linear fits (red lines). The insets show the emission at pH 6.7 and 12.1 under 365 nm UV light.

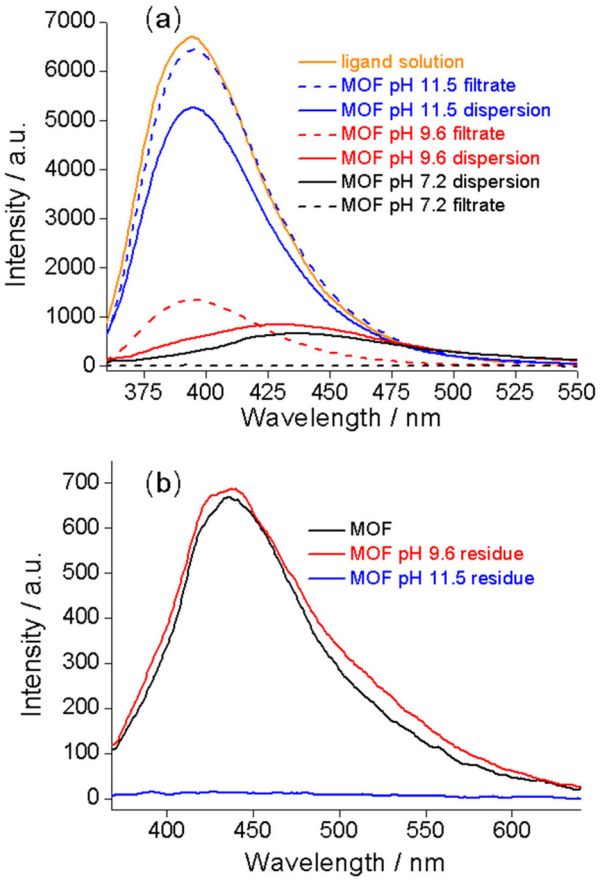

Fig. 2 (a) Emission spectra of Zr–TCPBP dispersed at different pH values (solid curves) and the corresponding filtrates (dashed curves). The spectrum of the $tcpbp^{4-}$ solution is included for comparison. (b) Emission spectra of different samples dispersed in neutral water. The samples include pristine Zr–TCPBP and the solid residue obtained by filtering the Zr–TCPBP dispersions at pH 9.6 and 11.5.

rated by analyzing the emission of the filter residues re-dispersed in neutral water. The residue from the pH 9.6 suspension shows almost identical emission to the as-synthesized MOF (Fig. 2b), suggesting that the framework is preserved with minor ligand leaching. However, the residue from the pH 11.5 dispersion is essentially non-fluorescent and shows no obvious IR bands attributable to the ligand (Fig. S2†), indicating almost complete hydrolysis of the MOF to zirconium hydroxide hydrate at the high pH.[27]

Based on the above analysis, the fluorescence variation of the MOF dispersion with pH can be well justified as follows. The pH-independent fluorescence in the pH 4.4–7.2 range comes from the MOF itself without ligand leaching. The fluorescence observed at an intermediate pH ($7.5 < pH < 11.5$) is an envelope of the emissions from the leached organic ligand and the retained MOF. The blue shift and intensity enhancement with pH are due to the short-wavelength and high-intensity contribution from the ligand becoming more and more significant. At $pH > 11.8$, the constant fluorescence is related to complete release of the ligands as a result of complete hydrolysis.

The pH-induced fluorescence change associated with partial to full basic hydrolysis inspired us to propose a fluorometric approach for characterizing the stability of MOFs in basic solutions. The hydrolysis occurs simply owing to the competition between the carboxylate group and increasing OH^- in binding metal ions at the node of the framework.[27] For Zr–TCPBP, the small intensity increment below pH 11 indicates that a small portion of the ligands is replaced by OH^-. The partial hydrolysis at nodes does not necessarily cause severe framework collapse, especially for the high-connectivity robust frameworks like Zr–TCPBP. The abrupt intensity rise above pH 11 indicates substantial ligand leaching because of the onset of the drastic destructive hydrolysis of the framework. The onset pH of the fluorescence change (ligand leaching) and the onset and critical pH for an abrupt fluorescence transition can be used as measures of the stability of the MOFs at different stages.

To verify the reliability of the fluorometric method, we examined the alkali stability of Zr–TCPBP by means of conventional solid-state characterization methods. The most widely used method is PXRD analysis with the solids isolated from dispersions. The method is unique for demonstrating the

retention of bulk crystallinity. Zr–TCPBP shows no significant change in PXRD after being soaked at pH up to 11 (30 mg of MOF in 10 mL of aqueous solution) (Fig. 3a, pH 11*). This seems to indicate that the MOF is stable at pH 11, but according to fluorescence analysis, there is actually significant leaching of the ligand at that pH. The conclusion drawn from PXRD actually depends on the amount of the MOF relative to the solution used. For 30 mg of MOF treated with 100 mL of solution (the concentration of the MOF is the same as that for fluorescence tests), the PXRD for pH 10.5 treatment becomes weaker especially for high-angle peaks (Fig. 3a). For pH 11, the PXRD worsens and shows only two broadened low-angle peaks, which indicates the preservation of only some degree of long-range order in the MOF. The sample treated at pH 11.5 shows a profile typical of amorphous solids, suggesting complete hydrolysis of the MOF. The results are consistent with fluorescence analysis, both confirming partial to complete hydrolysis as the pH is increased. However, the PXRD analysis is less sensitive and cannot definitely disclose the ligand leaching below pH 9.5, whereas the fluorescence analyses disclose the onset of leaching (hydrolysis) at pH 7.5. Furthermore, the facile pH-fluorescence titration analysis reveals an abrupt hydrolytic transition starting at pH 11 and completing at pH 11.8, with a critical pH of 11.4. The abrupt transition is difficult to identify and quantify with the PXRD method. In brief, the fluorometric method can be a simple but useful complement to PXRD for characterizing the stability of MOFs in basic solutions and provides more precise and detailed information of ligand leaching and framework decomposition.

SEM was used to analyze the morphology of the samples treated at different pH values (the concentration of the MOF is the same as that used in the fluorescence test). The as-synthesized sample of Zr–TCPBP contains uniform cubic crystallites of size about 400 nm (Fig. 4). There are no significant changes in the size and morphology after pH 9.5 treatment. This, in accordance with PXRD, confirms that the minor ligand leaching indicated by fluorescence analysis hardly affects the exterior appearance and the interior crystallinity, giving a framework with linker-vacancy defects. In other words, SEM is also less sensitive than the fluorometric method, which can detect a small degree of nondestructive local hydrolysis at Zr_6 nodes without framework collapse. At pH 10.5, the SEM images show a mixture of cubic, irregularly shaped and rough-surfaced particles of different sizes, indicating significant hydrolysis of the MOFs. At pH 11.5, the image is predominated by small, inhomogeneous and shapeless particles, confirming almost complete hydrolysis of the MOF. The morphological changes at pH 10.5 and 11.5 are consistent with the results obtained from PXRD and fluorescence analyses.

Thermal gravimetry (TG) was performed with the isolated solids to confirm the ligand leaching (Fig. S3†). The TG plots of Zr(IV) MOFs in air flow generally feature a plateau ascribable to the "dry" frameworks with dehydrated Zr_6O_6 nodes and multicarboxylate linkers, followed by rapid weight loss owing to linker decomposition and finally by a constant residual weight corresponding to ZrO_2.[42,47] The plateau/residual weight ratio can be used to estimate the linker/metal molar ratio. For pristine Zr–TCPBP, the TCPBP/Zr ratio was estimated to be

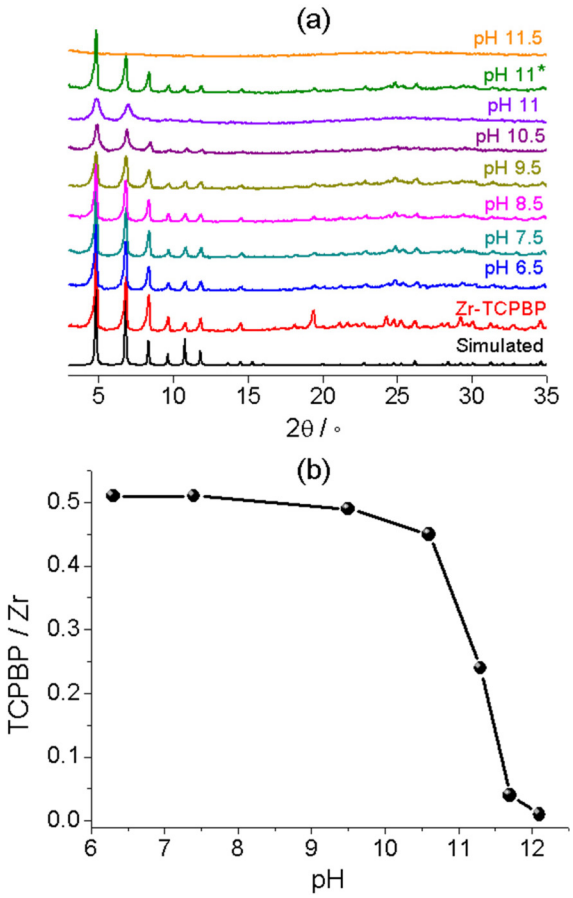

Fig. 3 (a) PXRD patterns of Zr–TCPBP treated with aqueous solutions at different pH values (30 mg of MOF with 100 mL of solution, except for pH 11*, for which 30 mg of MOF was treated with 10 mL of pH 11 solution). (b) TCPBP/Zr ratio obtained from TG analysis with the samples treated with aqueous solutions at different pH values.

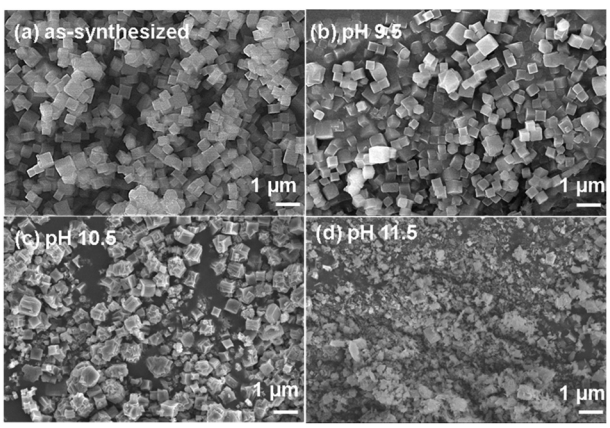

Fig. 4 SEM images of Zr–TCPBP. (a) As-synthesized. (b–d) Treated at different pH values.

0.51, very close to the 1 : 2 ratio expected for a defect-free structure. The linker/metal ratios for treated solids were plotted against pH at which the MOF was treated (Fig. 3b). As can be seen, the ratio does not change after treatment at near-neutral pH. The treatment at pH 9.5 (10.6) leads to a slight (obvious) decrease of the ratio, and an abrupt drop was witnessed for increasing pH from 10.6 to 11.7. The trend confirms the ligand leaching process disclosed by fluorescence analysis.

As mentioned earlier, the literature studies are divided based on the basic pH range in which UiO-66-NH_2 is stable.[42–44] Based on the above investigation with Zr–TCPBP, we believe that the discrepancy mainly arises from the different conditions for treating the MOF, especially the relative amount of the MOF to the solution, which has attracted little attention. We reassessed the basic hydrolytic stability of UiO-66-NH_2 by a combined study with fluorescence analysis, PXRD and SEM.

The emission spectra of UiO-66-NH_2 dispersed in aqueous solutions with pH 6.9–10.8 (0.1 mg mL^{-1}) are shown in Fig. 5a. The emission witnesses no shift in λ_{max} (425 nm) but a significant enhancement in the intensity with increasing pH. The intensity *versus* pH plot shows a slow increase for pH varying from 6.9 to 9.2, followed by an abrupt rise for pH 9.2–10.5, with the inflection point at pH 10.3 (Fig. 5b). The trend is similar to that observed for Zr–TCPBP, but the rapid intensity transition occurs at lower pH. This could indicate a low alkali resistance for UiO-66-NH_2. It is worth mentioning that a similar rapid fluorescence enhancement induced by a pH increase has been reported previously for UiO-66-NH_2 and also for its post-synthetically modified derivatives.[44] However, the authors ascribed the enhancement to the formation of the $-NH^-$ group by deprotonating the amino groups within the MOFs. To determine the real emissive species and the enhancement mechanism, the spectra of the supernatants obtained by filtering the dispersions were recorded (Fig. S4†). The spectra show the same λ_{max} as those observed for the dispersions, and the variation of emission intensity with pH is very similar to that for the dispersions (Fig. 5b). Notably, even at pH 6.9, the supernatant is fluorescent, with the intensity being slightly lower than that of the unfiltered suspension (Fig. S5†). The results strongly suggest that the emission predominantly arises from the linker leached to the liquid phase and that leaching occurs even at neutral pH. The emission from solid particles is minor. For further comparison, the aqueous solution of the linker, 2-aminoterephthalic acid, was investigated at various pH values. The results reveal that the linker at a fixed concentration shows pH-independent emission spectra in the range of pH 6.3–10.9, with λ_{max} = 425 nm (Fig. S6†). The invariant emission suggests invariant emissive species in the wide pH range. Referring to the pK_a values of comparable compounds (4.92 (–COOH) and 2.14 ($-NH_3^+$) for 2-aminobenzoic acid[48] and 3.20 and 4.30 for terephthalic acid[49]), the existing form of 2-aminoterephthalic acid in the above pH range should be the divalent anion with two carboxylic protons removed. Beyond the range, the fluorescence of the free linker decreases at pH ≥ 11.5 and is almost completely quenched at 13.2. This phenomenon can be ascribed to the deprotonation transformation from $-NH_2$ to $-NH^-$, consistent with the long-known example that aniline becomes non-fluorescent at pH > 13 for the same reason.[50] On the other hand, lowering the pH below 5.1 leads to a gradual red shift and intensity increase, which can be attributed to the gradual protonation of the divalent anion. Overall, the investigations with filtrates and the free linker definitely support that the

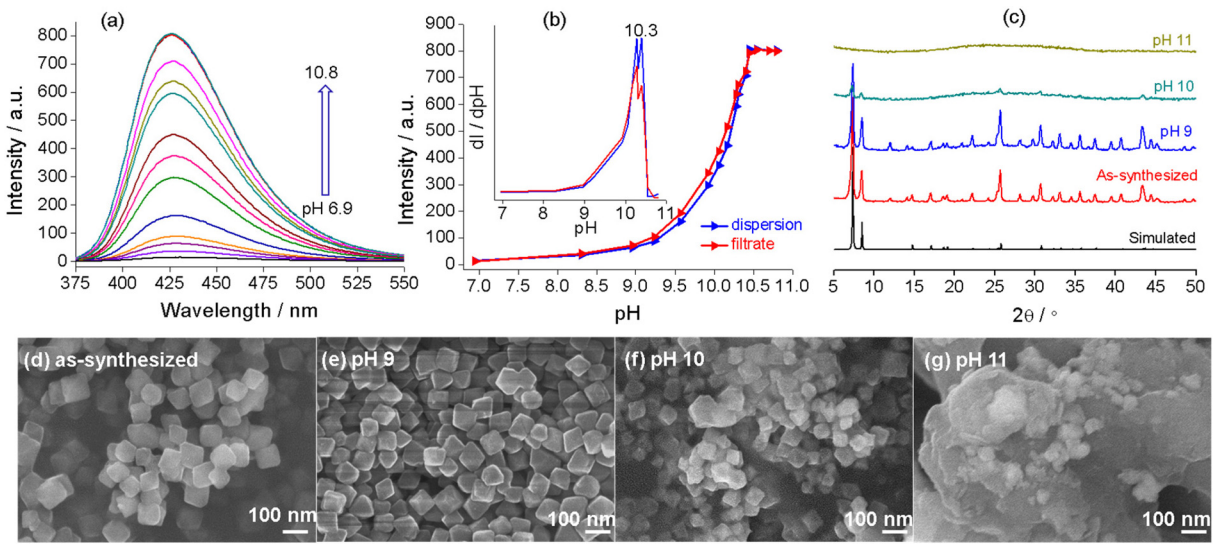

Fig. 5 (a) Emission spectra (320 nm excitation) of the dispersions of UiO-66-NH_2 under different pH conditions. (b) Emission intensity (425 nm) of the UiO-66-NH_2 aqueous dispersions of different pH values and their filtrates. The inset shows the derivative plot. (c) PXRD patterns of UiO-66-NH_2 treated with aqueous solutions of different pH values compared with the simulated pattern and that of the as-synthesized MOF. (d–g) SEM images of UiO-66-NH_2 before and after treatment at different pH values.

alkali-induced gradual and then abrupt emission enhancement for UiO-66-NH_2 is due to the increased linker leaching, or basic hydrolysis, rather than amino deprotonation. In particular, the fluorescence analysis reveals linker leaching even under neutral conditions and hydrolytic decomposition with a critical pH of 10.3. In addition, the kinetic measurements at various pH values suggest that the linker leaching and hydrolytic decomposition are fast and reach equilibrium within 10 min (Fig. S7†).

To validate and complement fluorescence analysis, PXRD and SEM were performed with the solid samples isolated after dispersing UiO-66-NH_2 in neutral to basic solutions (the solid-to-liquid ratio is the same as for fluorescence analysis). As shown in Fig. 5c, the sample after dispersion at pH = 9 displays a well-defined diffraction profile, and the SEM image shows uniform and discrete crystallites (Fig. 5e). There are no significant differences in the crystallinity and morphology as compared with pristine UiO-66-NH_2. The sample treated at pH 10 shows only a few weak diffraction peaks, and the particles become smaller and inhomogeneous and seem to be adhered together by the amorphous substance (Fig. 5f). For the sample treated at pH 11, SEM and PXRD confirm the formation of a featureless amorphous agglomerate (Fig. 5g). The above results confirm the rapid hydrolytic decomposition and ligand leaching above pH 9. The solid-state characterization methods give no information about ligand leaching at pH $\leq$ 9. Combining the dispersion fluorescence method and the solid-state methods, it can be concluded that partial ligand leaching (local hydrolysis at nodes) at a relatively low pH does not lead to significant degradation in the crystallinity and morphology. In addition, fluorescence titration analysis at high pH provides a facile method to determine the pH range for significant and complete hydrolytic decomposition.

Finally, it is worthwhile to emphasize the lessons learned from our study with Zr–TCPBP and UiO-66-NH_2. First, we should be cautious in judging the stability of MOFs towards chemical species in solutions from PXRD with the isolated solids. The PXRD results are strongly dependent not only on the concentration of the chemical species but also on the solid-to-liquid ratio used for treating MOFs (see Fig. 3a for Zr–TCPBP and Fig. S8† for UiO-66-NH_2). The latter factor has been largely neglected, which has led to inconsistent statements about the stability of MOFs. The PXRD method is incapable of detecting chemical leaching through nondestructive or even partially destructive processes. Second, fluorescence is sensitive to minor species. Many literature reports on fluorescence sensing have assigned the fluorescence (or stimulus-induced fluorescence change) of MOF suspensions to intact frameworks, based on stability characterization with PXRD.[51–53] Unfortunately, as indicated by this work, solid-state characterization methods are far from sufficient to warrant the assignment. To avoid a false understanding of the underlying chemistry and physics, careful examination of the liquid phases is required for identifying the real emissive/responsive species.

Conclusions

We have demonstrated the unique dual fluorescence response of Zr–TCPBP to basic pH by both wavelength shift and intensity enhancement. The mechanism has been proved to be associated with ligand leaching through nondestructive local hydrolysis to destructive framework hydrolysis. Based on the fluorescence response, we proposed and validated a fluorometric method to characterize the stability of MOFs towards alkaline solutions. The study was extended to UiO-66-NH_2, which preliminarily proved the universality of the method for luminescent MOFs or luminogenic MOFs. The method is simple, sensitive and informative. In particular, it can be a good complement to the conventional PXRD method and can be used to detect a small amount of ligand leaching to monitor the whole process from nondestructive local hydrolysis to obvious and complete destructive hydrolysis, and to determine the pH range for rapid decomposition. This method may be extended for characterizing the chemical stability of MOFs towards, for example, acids or other substrates of interest in solution. The combination of the sensitive fluorometric method with PXRD can help correct/avoid misunderstanding about the stability and especially the properties sensitive to chemical leaching.

Conflicts of interest

There are no conflicts to declare.

Acknowledgements

This work was supported by the National Natural Science Foundation of China (grants 21971069 and 21773070).

Notes and references

1 A. Kirchon, L. Feng, H. F. Drake, E. A. Joseph and H.-C. Zhou, From fundamentals to applications: a toolbox for robust and multifunctional MOF materials, *Chem. Soc. Rev.*, 2018, **47**, 8611–8638.
2 W.-H. Zhang, Z.-G. Ren and J.-P. Lang, Rational construction of functional molybdenum (tungsten)–copper–sulfur coordination oligomers and polymers from preformed cluster precursors, *Chem. Soc. Rev.*, 2016, **45**, 4995–5019.
3 S. Wang, C. M. McGuirk, A. d'Aquino, J. A. Mason and C. A. Mirkin, Metal-Organic Framework Nanoparticles, *Adv. Mater.*, 2018, **30**, e1800202.
4 T. Wang, E. Lin, Y.-L. Peng, Y. Chen, P. Cheng and Z. Zhang, Rational Design and Synthesis of Ultramicroporous Metal-organic Frameworks for Gas Separation, *Coord. Chem. Rev.*, 2020, **423**, 213485–213519.
5 L. Yang, Y. Wang, Y. Chen, J. Yang, X. Wang, L. Li and J. Li, Microporous metal-organic framework with specific functional sites for efficient removal of ethane from ethane/

ethylene mixtures, *Chem. Eng. J.*, 2020, **387**, 124137–124143.
6 J. B. De Coste and G. W. Peterson, Metal-Organic Frameworks for Air Purification of Toxic Chemicals, *Chem. Rev.*, 2014, **114**, 5695–5727.
7 D. Liu, J.-P. Lang and B. F. Abrahams, Highly Efficient Separation of a Solid Mixture of Naphthalene and Anthracene by a Reusable Porous Metal–Organic Framework through a Single-Crystal-to-Single-Crystal Transformation, *J. Am. Chem. Soc.*, 2011, **133**, 11042–11045.
8 Y. Zhang, S. Yuan, G. Day, X. Wang, X. Yang and H.-C. Zhou, Luminescent Sensors Based on Metal-organic Frameworks, *Coord. Chem. Rev.*, 2018, **354**, 28–45.
9 H.-Q. Yin and X.-B. Yin, Metal-Organic Frameworks with Multiple Luminescence Emissions: Designs and Applications, *Acc. Chem. Res.*, 2020, **53**, 485–495.
10 H.-Y. Li, S.-N. Zhao, S.-Q. Zang and J. Li, Functional metal-organic frameworks as effective sensors of gases and volatile compounds, *Chem. Soc. Rev.*, 2020, **49**, 6364–6401.
11 J. Dong, P. Shen, S. Ying, Z.-J. Li, Y. D. Yuan, Y. Wang, X. Zheng, S. B. Peh, H. Yuan, G. Liu, Y. Cheng, Y. Pan, L. Shi, J. Zhang, D. Yuan, B. Liu, Z. Zhao, B. Z. Tang and D. Zhao, Aggregation-Induced Emission-Responsive Metal–Organic Frameworks, *Chem. Mater.*, 2020, **32**, 6706–6720.
12 S. Khatua, S. Goswami, S. Biswas, K. Tomar, H. S. Jena and S. Konar, Stable Multiresponsive Luminescent MOF for Colorimetric Detection of Small Molecules in Selective and Reversible Manner, *Chem. Mater.*, 2015, **27**, 5349–5360.
13 N.-N. Yang, L.-J. Zhou, P. Li, Q. Sui and E.-Q. Gao, Space-confined indicator displacement assay inside a metal-organic framework for fluorescence turn-on sensing, *Chem. Sci.*, 2019, **10**, 3307–3314.
14 G. Li, S.-L. Yang, W.-S. Liu, M.-Y. Guo, X.-Y. Liu, R. Bu and E.-Q. Gao, Photoinduced versus spontaneous host–guest electron transfer within a MOF and chromic/luminescent response, *Inorg. Chem. Front.*, 2021, **8**, 4828–4837.
15 Y.-X. Shi, W.-H. Zhang, B. F. Abrahams, P. Braunstein and J.-P. Lang, Fabrication of Photoactuators: Macroscopic Photomechanical Responses of Metal-Organic Frameworks to Irradiation by UV Light, *Angew. Chem., Int. Ed.*, 2019, **58**, 9453–9458.
16 Y.-X. Shi, H.-H. Chen, W.-H. Zhang, G. S. Day, J.-P. Lang and H.-C. Zhou, Photoinduced nonlinear contraction behavior in metal-organic frameworks, *Chem. – Eur. J.*, 2019, **25**, 8543–8549.
17 A. Bavykina, N. Kolobov, I. S. Khan, J. A. Bau, A. Ramirez and J. Gascon, Metal-Organic Frameworks in Heterogeneous Catalysis: Recent Progress, New Trends, and Future Perspectives, *Chem. Rev.*, 2020, **120**, 8468–8535.
18 A. Karmakar and A. J. L. Pombeiro, Recent advances in amide functionalized metal organic frameworks for heterogeneous catalytic applications, *Coord. Chem. Rev.*, 2019, **395**, 86–129.
19 L.-J. Zhou, W. Sun, N.-N. Yang, P. Li, T. Gong, W.-J. Sun, Q. Sui and E.-Q. Gao, Facile and versatile "Click" approach toward multifunctional ionic metal-organic frameworks for efficient conversion of CO_2, *ChemSusChem*, 2019, **12**, 2202–2210.
20 M.-F. Wang, Y. Mi, F.-L. Hu, Z. Niu, X.-H. Yin, Q. Huang, H.-F. Wang and J.-P. Lang, Coordination-Driven Stereospecific Control Strategy for Pure Cycloisomers in Solid-State Diene Photocycloaddition, *J. Am. Chem. Soc.*, 2020, **142**, 700–704.
21 F.-L. Hu, Y. Mi, C. Zhu, B. F. Abrahams, P. Braunstein and J.-P. Lang, Stereoselective Solid-State Synthesis of Substituted Cyclobutanes Assisted by Pseudorotaxane-like MOFs, *Angew. Chem., Int. Ed.*, 2018, **57**, 12696–12701.
22 W.-H. Li, W.-H. Deng, G.-E. Wang and G. Xu, Conductive MOFs, *EnergyChem*, 2020, **2**, 100029.
23 D. W. Lim and H. Kitagawa, Rational strategies for proton-conductive metal-organic frameworks, *Chem. Soc. Rev.*, 2021, **50**, 6349–6368.
24 F. Yang, G. Xu, Y. Dou, B. Wang, H. Zhang, H. Wu, W. Zhou, J.-R. Li and B. Chen, A flexible metal–organic framework with a high density of sulfonic acid sites for proton conduction, *Nat. Energy*, 2017, **2**, 877–883.
25 Y.-B. Lu, Y.-Q. Liao, L. Dong, S.-D. Zhu, H.-R. Wen, J. Huang, X.-X. Dai, P. Lian, X.-M. Jiang, R. Li and Y.-R. Xie, Ultra-Stable Metal–Organic Framework with Concurrent High Proton Conductivity and Fluorescence Sensing for Nitrobenzene, *Chem. Mater.*, 2021, **33**, 7858–7868.
26 L. Feng, K.-Y. Wang, G. S. Day, M. R. Ryder and H.-C. Zhou, Destruction of Metal-Organic Frameworks: Positive and Negative Aspects of Stability and Lability, *Chem. Rev.*, 2020, **120**, 13087–13133.
27 S. Yuan, L. Feng, K. Wang, J. Pang, M. Bosch, C. Lollar, Y. Sun, J. Qin, X. Yang, P. Zhang, Q. Wang, L. Zou, Y. Zhang, L. Zhang, Y. Fang, J. Li and H.-C. Zhou, Stable Metal-Organic Frameworks: Design, Synthesis, and Applications, *Adv. Mater.*, 2018, **30**, 1704303.
28 D. Buzek, J. Demel and K. Lang, Zirconium Metal-Organic Framework UiO-66: Stability in an Aqueous Environment and Its Relevance for Organophosphate Degradation, *Inorg. Chem.*, 2018, **57**, 14290–14297.
29 D. Buzek, S. Adamec, K. Lang and J. Demel, Metal-organic frameworks vs. buffers: case study of UiO-66 stability, *Inorg. Chem. Front.*, 2021, **8**, 720–734.
30 Y. Liu, X.-Y. Xie, C. Cheng, Z.-S. Shao and H.-S. Wang, Strategies to fabricate metal–organic framework (MOF)-based luminescent sensing platforms, *J. Mater. Chem. C*, 2019, **7**, 10743–10763.
31 G.-L. Yang, X.-L. Jiang, H. Xu and B. Zhao, Applications of MOFs as Luminescent Sensors for Environmental Pollutants, *Small*, 2021, **17**, 2005327.
32 J. Jin, J. Xue, Y. Liu, G. Yang and Y.-Y. Wang, Recent progresses in luminescent metal-organic frameworks (LMOFs) as sensors for the detection of anions and cations in aqueous solution, *Dalton Trans.*, 2021, **50**, 1950–1972.
33 S. Wu, H. Min, W. Shi and P. Cheng, Multicenter Metal-Organic Framework-Based Ratiometric Fluorescent Sensors, *Adv. Mater.*, 2020, **32**, 1805871.

34 C.-Y. Liu, X.-R. Chen, H.-X. Chen, Z. Niu, H. Hirao, P. Braunstein and J.-P. Lang, Ultrafast Luminescent Light-Up Guest Detection Based on the Lock of the Host Molecular Vibration, *J. Am. Chem. Soc.*, 2020, **142**, 6690–6697.

35 T.-Y. Gu, M. Dai, D. J. Young, Z.-G. Ren and J.-P. Lang, Luminescent Zn(II) Coordination Polymers for Highly Selective Sensing of Cr(III) and Cr(VI) in Water, *Inorg. Chem.*, 2017, **56**, 4668–4678.

36 J. H. Cavka, S. Jakobsen, U. Olsbye, N. Guillou, C. Lamberti, S. Bordiga and K. P. Lillerud, A New Zirconium Inorganic Building Brick Forming Metal Organic Frameworks with Exceptional Stability, *J. Am. Chem. Soc.*, 2008, **130**, 13850–13851.

37 M. Bosch, M. Zhang and H.-C. Zhou, Increasing the Stability of Metal-Organic Frameworks, *Adv. Chem.*, 2014, **2014**, 182327.

38 B. Wang, Q. Yang, C. Guo, Y. Sun, L.-H. Xie and J.-R. Li, Stable Zr(IV)-Based Metal-Organic Frameworks with Predesigned Functionalized Ligands for Highly Selective Detection of Fe(III) Ions in Water, *ACS Appl. Mater. Interfaces*, 2017, **9**, 10286–10295.

39 X.-L. Lv, S. Yuan, L.-H. Xie, H. F. Darke, Y. Chen, T. He, C. Dong, B. Wang, Y.-Z. Zhang, J.-R. Li and H.-C. Zhou, Ligand Rigidification for Enhancing the Stability of Metal-Organic Frameworks, *J. Am. Chem. Soc.*, 2019, **141**, 10283–10293.

40 H.-L. Jiang, D. Feng, K. Wang, Z.-Y. Gu, Z. Wei, Y.-P. Chen and H.-C. Zhou, An Exceptionally Stable, Porphyrinic Zr Metal-Organic Framework Exhibiting pH-Dependent Fluorescence, *J. Am. Chem. Soc.*, 2013, **135**, 13934–13938.

41 N. Huang, S. Yuan, H. Drake, X. Yang, J. Pang, J. Qin, J. Li, Y. Zhang, Q. Wang, D. Jiang and H.-C. Zhou, Systematic Engineering of Single Substitution in Zirconium Metal-Organic Frameworks toward High-Performance Catalysis, *J. Am. Chem. Soc.*, 2017, **139**, 18590–18597.

42 M. Kandiah, M. H. Nilsen, S. Usseglio, S. Jakobsen, U. Olsbye, M. Tilset, C. Larabi, E. A. Quadrelli, F. Bonino and K. P. Lillerud, Synthesis and Stability of Tagged UiO-66 Zr-MOFs, *Chem. Mater.*, 2010, **22**, 6632–6640.

43 K. Leus, T. Bogaerts, J. De Decker, H. Depauw, K. Hendrickx, H. Vrielinck, V. Van Speybroeck and P. Van Der Voort, Systematic study of the chemical and hydrothermal stability of selected "stable" Metal Organic Frameworks, *Microporous Mesoporous Mater.*, 2016, **226**, 110–116.

44 J. Aguilera-Sigalat and D. Bradshaw, A colloidal water-stable MOF as a broad-range fluorescent pH sensor via post-synthetic modification, *Chem. Commun.*, 2014, **50**, 4711–4713.

45 S.-L. Yang, G. Li, M.-Y. Guo, W.-S. Liu, R. Bu and E.-Q. Gao, Positive Cooperative Protonation of a Metal-Organic Framework: pH-Responsive Fluorescence and Proton Conduction, *J. Am. Chem. Soc.*, 2021, **143**, 8838–8848.

46 X.-L. Lv, L.-H. Xie, B. Wang, M. Zhao, Y. Cui and J.-R. Li, Flexible metal-organic frameworks for the wavelength-based luminescence sensing of aqueous pH, *J. Mater. Chem. C*, 2018, **6**, 10628–10639.

47 C. G. Piscopo, A. Polyzoidis, M. Schwarzer and S. Loebbecke, Stability of UiO-66 under acidic treatment: Opportunities and limitations for post-synthetic modifications, *Microporous Mesoporous Mater.*, 2015, **208**, 30–35.

48 M. S. K. Niazi and J. Mollin, Dissociation Constants of Some Amino Acid and Pyridinecarboxylic Acids in Ethanol–H_2O Mixtures, *Bull. Chem. Soc. Jpn.*, 1987, **60**, 2605–2610.

49 J. M. Vandenbelt, C. Henrich and S. G. Vanden Berg, Comparison of pKá Values Determined by Electrometric Titration and Ultraviolet Absorption Methods, *Anal. Chem.*, 1954, **26**, 726–727.

50 J. W. Bridges and R. T. Williams, Fluorescence of indoles and aniline derivatives, *Biochem. J.*, 1968, **107**, 225–237.

51 S.-L. Hou, J. Dong, M.-H. Tang, X.-L. Jiang, Z.-H. Jiao and B. Zhao, Triple-Interpenetrated Lanthanide-Organic Framework as Dual Wave Bands Self-Calibrated pH Luminescent Probe, *Anal. Chem.*, 2019, **91**, 5455–5460.

52 J. Wang, Y. Li, M. Jiang, Y. Liu, L. Zhang and P. Wu, A Highly Chemically Stable Metal-Organic Framework as a Luminescent Probe for the Regenerable Ratiometric Sensing of pH, *Chem. – Eur. J.*, 2016, **22**, 13023–13027.

53 K. Xing, R. Fan, F. Wang, H. Nie, X. Du, S. Gai, P. Wang and Y. Yang, Dual-Stimulus-Triggered Programmable Drug Release and Luminescent Ratiometric pH Sensing from Chemically Stable Biocompatible Zinc Metal-Organic Framework, *ACS Appl. Mater. Interfaces*, 2018, **10**, 22746–22756.